



STRUCTURAL SCIENCE
CRYSTAL ENGINEERING
MATERIALS

1

2 **Volume 71 (2015)**

3 **Supporting information for article:**

4 **On the transferability of electron density in EleEebinary vanadium
5 borides VB, V₃B₄ and VB₂**

6 **Bürgehan Terlan, Lev Akselrud, Alexey I. Baranov, Horst Borrman and Yuri
7 Grin**

8

9

1 **Table S1** Atomic coordinates and displacement parameters of VB_2 , VB and V_3B_4

Parameters	VB_2		VB		V_3B_4			
	V (6/mmm)	B ($\bar{6}m2$)	V (m2m)	B (m2m)	V1 (mmm)	V2 (mm2)	B1 (mm2)	B2 (mm2)
x	0	1/3	0	0	0	1/2	0	1/2
y	0	2/3	0.14750(2)	0.43757(7)	0	0	0	0
z	0	1/2	1/4	1/4	0	0.31247(1)	0.43450(4)	0.13649(5)
B_{11} (\AA^2)	0.115(3)	0.217(4)	0.125(4)	0.312(10)	0.119(5)	0.124(5)	0.28(1)	0.31(2)
B_{22} (\AA^2)	B_{11}	B_{11}	0.105(4)	0.310(10)	0.155(5)	0.185(4)	0.32(2)	0.30(1)
B_{33} (\AA^2)	0.133(4)	0.341(7)	0.121(4)	0.269(9)	0.161(5)	0.151(4)	0.261(9)	0.33(1)
B_{12} (\AA^2)	$\frac{1}{2} B_{11}$	$\frac{1}{2} B_{11}$	-	-	-	-	-	-
D_{III1} (\AA^4)	3.219(192)		1.665(127)		1.504(281)	0.538(251)		
D_{IIII}			-0.034(3)		-	-	-	-
D_{2222} (\AA^4)					1.914(206)	0.448(172)		
D_{3333} (\AA^4)	2.011(133)		1.641(142)		-	-	-	-
D_{II12} (\AA^4)	$\frac{1}{2} D_{IIII}$	-	-	-	-	-	-	-
D_{I222} (\AA^4)	$\frac{1}{2} D_{IIII}$	-	-	-	-	-	-	-
D_{II22} (\AA^4)	$\frac{1}{2} D_{IIII}$	-	-0.079(6)	-	-0.586(79)	-0.296(59)	-	-
D_{II33} (\AA^4)	-0.729(48)	-	-0.494(44)	-	-0.031(4)	-0.015(3)	-	-
D_{2233} (\AA^4)	D_{II33}	-	-0.085(6)	-	-0.014(4)	-0.007(3)	-	-
D_{I233} (\AA^4)	$\frac{1}{2} D_{II33}$	-	-	-	-	-	-	-

2
3
4
5
6
7
8
9
10
11
12
13

1 **Table S2** Topological characteristics of cps determined from reconstructed experimental and
 2 theoretically calculated ED in VB_2 . Theoretical values are denoted by an asterisk. Variations for $\rho(r_{\text{cp}})$
 3 and $\nabla^2\rho(r_{\text{cp}})$ at the associated critical points between theory and experiment are in the range of ± 0.088
 4 $e \text{ \AA}^{-3}$ and $\pm 0.767 e \text{ \AA}^{-5}$, respectively.

Interaction	Type of cp	Wyckoff notation and position of cp	$\rho(r_{\text{cp}})$ (e \AA^{-3})	$\nabla^2\rho(r_{\text{cp}})$ (e \AA^{-5})	λ_1 (e \AA^{-5})	λ_2 (e \AA^{-5})	λ_3 (e \AA^{-5})
B-B	3, -1	3(g)(0.5,0.5,0.5)	0.82(2)	-3.71(2)	-3.38	-1.92	1.59
	3, -1	3(g)(0.5,0.5,0.5)*	0.83	-4.48	-3.12	-2.76	1.40
B-V	3, -1	12(o)(0.820, 0.180, 0.232)	0.37(1)	3.02(2)	-0.96	-0.11	4.10
	3, -1	12(o)(0.833, 0.167, 0.261)*	0.39	2.30	-1.07	-0.20	3.57
	3, +1	12(n)(0, 0.688, 0.237)	0.36(1)	2.83(2)	-0.93	0.12	3.64
	3, +1	12(n)(0, 0.713, 0.267)*	0.38	2.43	-1.03	0.18	3.27
	3, +1	3(f)(0, 0.5, 0)	0.24(5)	1.05(1)	-0.04	0.47	0.62
	3, +1	3(f)(0, 0.5, 0)*	0.22	1.05	-0.07	0.52	0.60
	3, +3	2(c)(0.333, 0.667, 0)	0.24(7)	1.02(1)	0.05	0.05	0.93
	3, +3	2(c)(0.333, 0.667, 0)*	0.21	0.95	0.07	0.07	0.81
	3, +3	1(b)(0,0,0.5)	0.12(6)	1.70(1)	0.48	0.48	0.75
	3, +3	1(b)(0,0,0.5)*	0.21	1.42	0.55	0.55	0.33

5
 6
 7
 8
 9
 10
 11
 12
 13
 14
 15

1 **Table S3** Topological characteristics of cps determined from reconstructed experimental and
 2 theoretically calculated ED in VB. Theoretical values are denoted by an asterisk. Variations for $\rho(r_{cp})$
 3 and $\nabla^2\rho(r_{cp})$ at the associated critical points between theory and experiment are in the range of ± 0.073
 4 e Å⁻³ and ± 1.339 e Å⁻⁵, respectively.

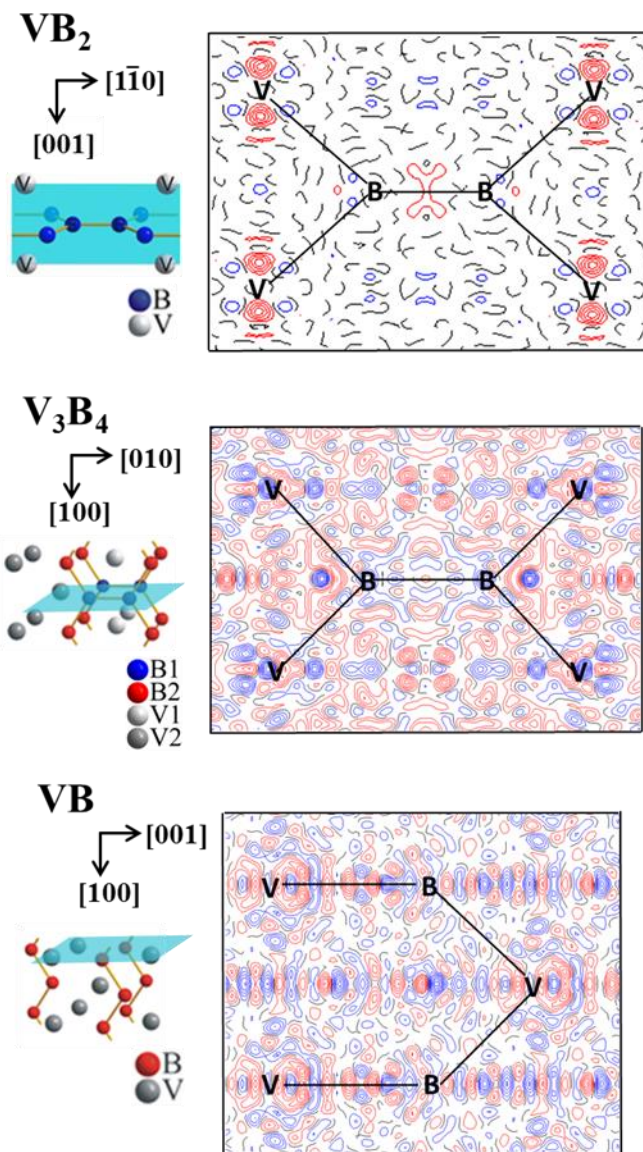
Interaction	Type of cp	Wyckoff notation and position of cp	$\rho(r_{cp})$ (e Å ⁻³)	$\nabla^2\rho(r_{cp})$ (e Å ⁻⁵)	λ_1 (e Å ⁻⁵)	λ_2 (e Å ⁻⁵)	λ_3 (e Å ⁻⁵)
B-B	3, -1	4(b)(0.5, 0.0, 0.5)	0.76(2)	-1.41(12)	-2.26	-1.99	2.84
	3, -1	4(b)(0.5, 0.0, 0.5)*	0.74	-2.75	-2.36	-2.01	1.62
B-V	3, -1	16(h)(0.249, -0.086, 0.496)	0.42(7)	3.00(7)	-1.06	-0.59	4.65
	3, -1	16(h)(0.242, -0.007, 0.499)*	0.43	2.13	-1.16	-0.62	3.92
	3, -1	8(g)(0.252, 0.037, 0.250)	0.41(11)	3.37(12)	-0.88	-0.14	4.39
	3, -1	8(g)(0.243, 0.040, 0.250)*	0.41	2.50	-0.95	-0.19	3.64
	3, -1	4(c)(0, -0.283, 0.75)	0.31(17)	3.45(14)	-0.89	-0.16	4.57
	3, -1	4(c)(0, -0.291, 0.75)*	0.38	2.29	-0.58	-0.65	3.52
	3, +1	16(h)(0.262, -0.046, 0.633)	0.40(9)	3.08(9)	-0.87	0.23	3.71
5 6 7 8 9 10 11 12 13 14 15 16	3, +1	16(h)(0.267, -0.050, 0.641)*	0.40	2.63	-0.93	0.26	3.29
	3, +1	8(d)(0.25, -0.25, 0.50)	0.21(2)	1.01(1)	-0.34	0.17	1.18
	3, +1	8(d)(0.25, -0.25, 0.50)*	0.28	1.20	-0.36	0.02	1.55
	3, +1	4(a)(0, 0, 0.5)	0.28(2)	2.15(2)	-0.28	0.18	2.25
	3, +1	4(a)(0, 0, 0.5)*	0.27	1.27	-0.10	0.43	0.94
	3, +3	4(c)(0.5, -0.250, 0.75)	0.17(1)	0.40(1)	0.002	0.12	0.25
	3, +3	4(c)(0.5, -0.386, 0.75)*	0.21	0.52	0.26	0.06	0.20

1 **Table S4** Topological characteristics of cps determined from reconstructed experimental and
 2 theoretically calculated ED in V_3B_4 . Theoretical values are denoted by an asterisk. Variations for
 3 $\rho(r_{cp})$ and $\nabla^2\rho(r_{cp})$ at the associated critical points between theory and experiment are in the range of
 4 $\pm 0.064 \text{ e } \text{\AA}^{-3}$ and $\pm 2.295 \text{ e } \text{\AA}^{-5}$, respectively.

Interaction	Type of cp	Wyckoff notation and position of cp	$\rho(r_{cp})$ (e \AA^{-3})	$\nabla^2\rho(r_{cp})$ (e \AA^{-5})	λ_1 (e \AA^{-5})	λ_2 (e \AA^{-5})	λ_3 (e \AA^{-5})
B-B	3, -1	2(c)(0.5, 0.5, 0)	0.86(6)	-2.35(6)	-3.14	-2.44	3.22
	3, -1	2(c)(0.5, 0.5, 0)*	0.81	-4.12	-2.92	-2.66	1.46
	3, -1	8(l)(0.5, 0.246, 0.100)	0.77(1)	-1.24(4)	-2.33	-2.25	3.33
	3, -1	8(l)(0.5, 0.249, 0.103)*	0.79	-3.54	-2.72	-2.34	1.52
B-V	3, -1	8(m)(0.260, 0, 0.377)	0.43(8)	4.34(4)	-0.87	-0.68	5.90
	3, -1	8(m)(0.237, 0, 0.375)*	0.45	2.49	-1.31	-0.39	4.18
	3, -1	16(o)(0.258, 0.270, 0.151)	0.39(8)	3.70(3)	-0.70	-0.33	4.74
	3, -1	16(o)(0.264, 0.260, 0.155)*	0.44	2.27	-1.28	-0.42	3.96
	3, -1	16(o)(0.255, 0.271, 0.026)	0.39(5)	3.44(3)	-0.79	-0.28	4.51
	3, -1	16(o)(0.258, 0.256, 0.032)*	0.39	2.25	-1.00	-0.30	3.55
	3, -1	4(j) (0.5, 0, 0.226)	0.34(16)	2.87(8)	-0.78	-0.73	4.37
	3, -1	4(j) (0.5, 0, 0.225)*	0.38	2.27	-0.71	-0.58	3.57
	3, -1	8(m)(0.244, 0, 0.068)	0.37(7)	3.41(4)	-0.70	-0.29	4.39
	3, -1	8(m)(0.256, 0, 0.068)*	0.36	2.23	-0.80	-0.05	3.08
V-V	3, +1	16(o)(0.270, 0.319, 0.141)	0.390(7)	3.69(2)	-0.70	0.33	4.06
	3, +1	16(o)(0.275, 0.343, 0.138)*	0.43	2.72	-1.20	0.23	3.62
	3, +1	8(n)(0.267, 0.290, 0)	0.38(6)	3.23(3)	-0.81	0.22	3.82
	3, +1	8(n)(0.272, 0.283, 0)*	0.38	2.51	-0.99	0.23	3.27
	3, +1	16(o)(0.269, 0.130, 0.059)	0.35(6)	3.16(2)	-0.68	0.35	3.49
	3, +1	16(o)(0.259, 0.063, 0.067)*	0.36	2.28	-0.79	0.08	2.99
	3, +1	8(k)(0.25, 0.25, 0.25)	0.21(2)	1.41(1)	-0.24	0.10	1.54
	3, +1	8(k)(0.25, 0.25, 0.25)*	0.28	1.20	-0.38	0.04	1.55
	3, +1	8(l)(0.5, 0.104, 0.450)	0.26(4)	1.24(2)	-0.19	0.55	0.87
	3, +1	8(l)(0.5, 0.213, 0.328)*	0.24	1.13	-0.08	0.55	0.67
	3, +1 [†]	4(l)(0.5, 0.5, 0.328)*	0.24	0.974	-0.06	0.36	0.68
	3, +3 [†]	4(l)(0.5, 0.5, 0.379)*	0.21	0.97	0.04	0.14	0.79
	3, +3	2(d)(0, 0.5, 0)	0.24(2)	1.06(2)	0.17	0.21	0.68
	3, +3	2(d)(0, 0.5, 0)*	0.22	1.10	0.06	0.47	0.57
	3, +3	2(b)(0.5, 0, 0)	0.23(4)	1.17(3)	0.34	0.38	0.44
	3, +3	2(b)(0.5, 0, 0)*	0.21	1.31	0.36	0.39	0.56
	3, +3	4(l)(0.5, 0.5, 0.262)	0.17(1)	0.48(1)	0.14	0.15	0.17
	3, +3	4(l)(0.5, 0.5, 0.224)*	0.21	0.58	0.07	0.23	0.28

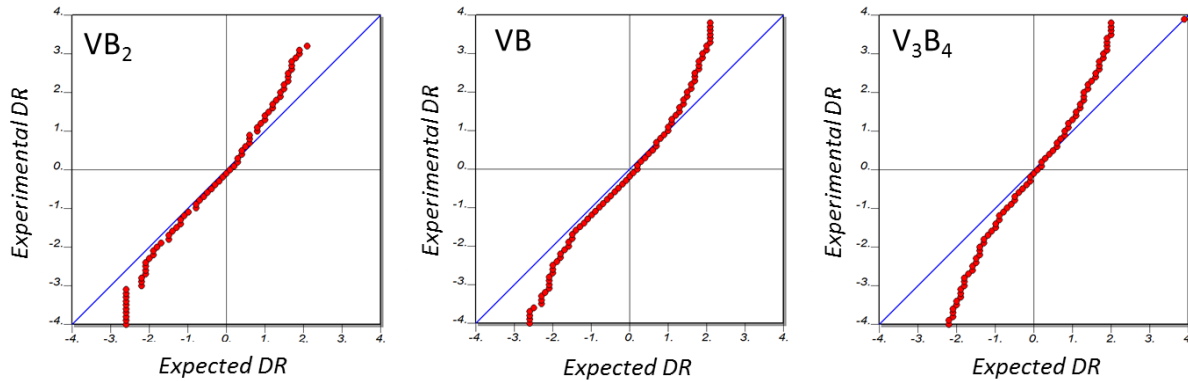
5 [†] (3,+1) and (3,+3) cps at the 4(l) positions are not observed by experiment.

1 **Figure S1** Residual density maps of VB_2 , VB and V_3B_4 after multipole refinement in planes as
2 shown up to the experimental resolution ($\sin \theta / \lambda \leq 1.65 \text{ \AA}^{-1}$, $\sin \theta / \lambda \leq 1.65 \text{ \AA}^{-1}$ and $\sin \theta / \lambda \leq 1.55$
3 \AA^{-1} , respectively. Contour level step width is 0.1 e \AA^{-3} . Red and blue lines correspond to positive and
4 negative values, whereas dashed solid line is the zero contour. The maximum and minimum values of
5 the residual densities are $0.48 / -0.17 \text{ \AA}^{-3}$ for VB_2 , $0.66 / -0.87 \text{ e \AA}^{-3}$ for VB , and $0.81 / -0.81 \text{ e \AA}^{-3}$ for
6 V_3B_4 , respectively.



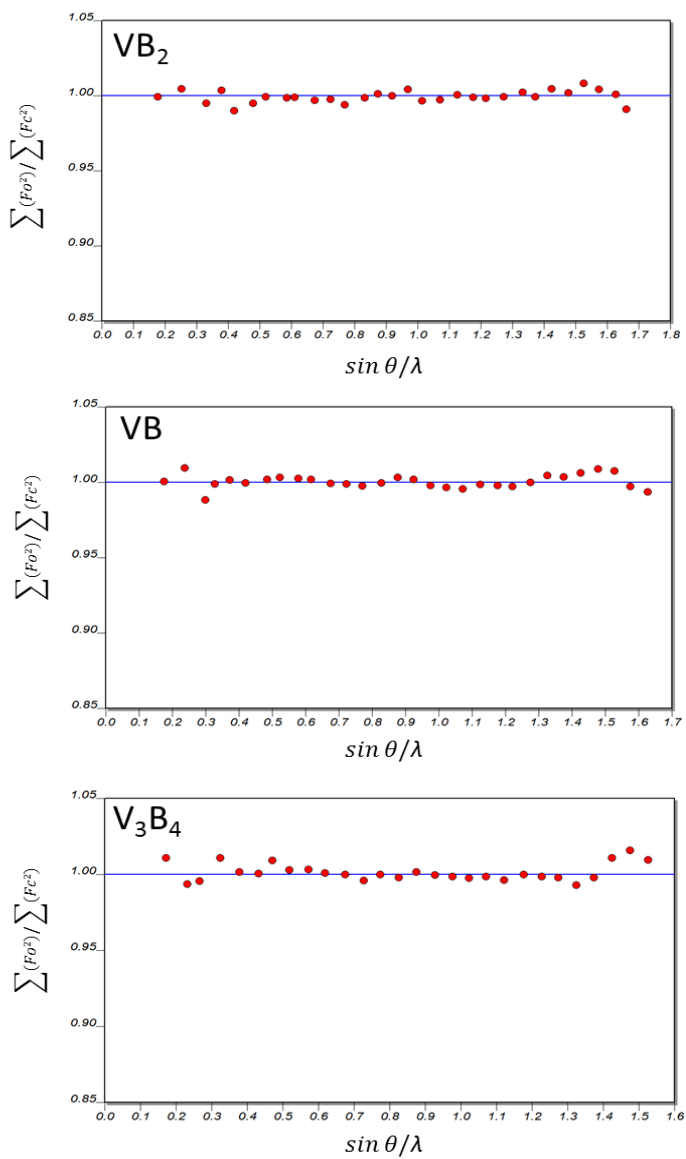
7
8
9
10
11

1 **Figure S2** Normal probability plots for the residual density from multipole modelling of
2 experimental data for VB_2 , VB and V_3B_4 up to the experimental resolution ($\sin \theta/\lambda \leq 1.65 \text{ \AA}^{-1}$, (\sin
3 $\theta/\lambda \leq 1.65 \text{ \AA}^{-1}$ and ($\sin \theta/\lambda \leq 1.55 \text{ \AA}^{-1}$, respectively.



4
5
6
7
8
9
10
11
12
13
14
15
16
17
18
19
20
21
22
23
24
25
26
27
28

1 **Figure S3** Scale factor variation from multipole modelling of experimental data averaged for VB_2 ,
2 VB and V_3B_4 up to the experimental resolution ($\sin \theta/\lambda \leq 1.65 \text{ \AA}^{-1}$, ($\sin \theta/\lambda \leq 1.65 \text{ \AA}^{-1}$ and ($\sin \theta/\lambda \leq$
3 1.55 \AA^{-1} , respectively.



4
5
6
7
8
9
10
11

1 **Figure S4** Meindl plots: Fractal dimension (d^f) versus residual density ρ_o ($e \text{ \AA}^{-3}$) for the multipole
2 refinement of VB_2 , VB and V_3B_4 up to the experimental resolution ($\sin \theta/\lambda \leq 1.65 \text{ \AA}^{-1}$, ($\sin \theta/\lambda \leq 1.65$
3 \AA^{-1} and ($\sin \theta/\lambda \leq 1.55 \text{ \AA}^{-1}$, respectively.

